ChemistrySelect

Research Article
doi.org/10.1002/slct.202204191

Chemistry Europe
European Chemical Societies Publishing

www.chemistryselect.org

Carboxylate- and Sulfonate-Containing Quinazolin-4(3H)-one Rings: Synthesis, Characterization, and Carbonic Anhydrase I–II and Acetylcholinesterase Inhibition Properties

Feyzi Sinan Tokalı,[a] Zuhal Alım,*[b] and Ümit Yırtıcı[c]

Quinazolines are a group of bioactive heterocyclic compounds with a wide range of biological activities and have gained an important place in the design of active drugs with various targets due to their pharmacological properties. Carbonic anhydrase (CA) and acetylcholinesterase (AChE) inhibitors are very important pharmacologically. In this study, inhibition effects of newly synthesized quinazolin-4(3*H*)-one derivatives on human erythrocyte CA-I (hCA-I) and CA-II (hCA-II) isoenzyme and AChE activity were investigated. The structures of the novel compounds were characterized by fourier-transform infrared (FTIR), nuclear magnetic resonance (NMR), and high-resolution mass spectroscopy (HRMS). All molecules showed strong inhibitory effect in all three enzymes. 4-[(4-Oxo-2-(phenoxymethyl)quinazolin-3(4*H*)-ylimino)methyl]phenyl furan-2-carboxylate for hCA-I (IC_{50}: 205 nM), 4-[(4-oxo-2-(phenoxymethyl)quinazolin-3(4*H*)-ylimino)methyl]phenyl isobutyrate for hCA-II (IC_{50}: 209 nM), and 4-[(4-oxo-2-(phenoxymethyl)quinazolin-3(4*H*)-ylimino)methyl]phenyl propionate for AChE (IC_{50}: 14.2 nM) were the molecules that showed the strongest inhibitory effect. Molecular docking studies were carried out to elucidate the possible interaction mechanism of the molecules in the active site of the enzymes. The affinity scores of the most active compounds for hCA-I, hCA-II, and AChE were determined as −134.765, −147.423, and −175.354 MolDock Score, respectively.

Introduction

Carbonic anhydrase (CA, EC 4.2.1.1) is a zinc-dependent metalloenzyme from the lyase group, which is very common in prokaryotic and eukaryotic organisms.[1] It plays an important role in many physiological and pathological processes, such as pH balance, electrolyte secretion, bone resorption, calcification, gluconeogenesis, and tumor formation, by catalyzing the reversible reaction in which CO_2 is converted to bicarbonate (HCO_3^-) and proton (H^+).[2,3,4] To date, eight different CA families have been categorized as α-CAs, β-CAs,γ-CAs,δ-CAs,ζ-CAs,η-CAs,θ-CAs, and t-CAs.[5] Of these isoforms, only α-CAs are found in humans, and 16 isoenzymes (hCAI-hCAXVI) are present. Of these isoenzymes, hCAVIII, hCAX, and hCAXI do not have catalytic activity. The CAII isoenzyme has the highest catalytic activity (Kcat/Km 1.5×10^8 $M^{-1}s^{-1}$), and the distribution of these 16 isoenzymes in tissues, their catalytic activities, and their affinities for inhibitors and activators differ.[1,4,6,7] Since CA isoenzymes are associated with many pathological conditions such as obesity, epilepsy, Alzheimer's, cancer, glaucoma, hemolyticanemia, osteoporosis, and neuropathic pain, the determination of specific inhibitors of these isoenzymes has attracted the attention of scientific studies. Today, assorted CA inhibitors such as Acetazolamide (AZA), Methazolamide, Dorzolamide, Brinzolamide, Diclofenamide, Ethoxazolamide, Zonisamide, Indisulam, etc. are available. However, the fact that these inhibitors are not selective and have undesirable side effects

Table 1. Inhibition results for hCA-I and hCAII.

Compounds	hCA-I IC_{50} (nM)	R^2	hCA-II IC_{50} (nM)	R^2
1	3320	0.9200	3910	0.9271
2	371	0.9228	312	0.9801
3	616	0.9311	209	0.9801
4	453	0.9587	272	0.9468
5	342	0.9353	232	0.9640
6	205	0.9509	485	0.9635
7	592	0.9734	692	0.9540
8	484	0.9648	556	0.9798
9	444	0.9855	399	0.8963
10	518	0.9946	626	0.9787
11	290	0.9412	473	0.9618
12	282	0.9646	533	0.9889
13	368	0.9859	530	0.8445
14	475	0.9623	431	0.9523
15	453	0.9930	510	0.9701
16	550	0.9597	271	0.9693
Acetazolamide (AZA)[a]	476	0.9836	104	0.9571

[a] Acetazolamide (AZA) was used as a standard inhibitor for hCA-I and hCA-II.

[a] *F. S. Tokalı*
Department of Material and Material Processing Technologies,
Kars Vocational School, Kafkas University,
Kars, Turkey
[b] *Prof. Dr. Z. Alım*
Department of Chemistry, Faculty of Arts and Sciences,
Kırşehir Ahi Evran University, Kırşehir, Turkey
E-mail: zuhal.alim@ahievran.edu.tr
[c] *Ü. Yırtıcı*
Department of Medical Laboratory,
Kırıkkale University, Kırıkkale, Turkey

Supporting information for this article is available on the WWW under https://doi.org/10.1002/slct.202204191

Table 2. Inhibition results for AChE.

Compounds	AChE IC_{50} (nM)	R^2
1	45.8	0.9529
2	14.2	0.9234
3	148.0	0.9135
4	139.0	0.9367
5	70.8	0.9339
6	108.0	0.9073
7	21.8	0.9375
8	119.0	0.9072
9	69.5	0.9443
10	114.0	0.9316
11	108.0	0.9201
12	106.0	0.9085
13	155.0	0.9426
14	57.4	0.9711
15	50.2	0.9521
16	125.0	0.9850
Tacrine (TAC)[a]	210.0	0.9152

has necessitated the discovery of new, effective, isoenzyme-specific CA inhibitors.[4,8,9] The sulfonamide group is the most important and leading CA inhibitor group.[10,11] In addition, the CA inhibition effects of various molecular derivatives such as pyrazolin/pyrazole,selenols, purine/pyrimidine, phthazoline, imidazole, oxadiazole, quinazoline, indole were determined in recent studies[1] and studies to identify new CA inhibitors are continuing rapidly.

Alzheimer's disease (AD) is the most common neuro-degenerative disorder in the elderly, causing loss of vital functions such as memory loss, speech deficiency, cognitive function, and behavioural disorders.[12,13] The number of AD patients, which is one of the main causes of death in the elderly, is increasing all over the World.[14] Although there is currently no definitive treatment for AD, drug development studies have focused on acetylcholinesterase (AChE) inhibition to treat this disease.[15] AChE removes acetylcholine (ACh) from the synaptic gap by catalyzing the hydrolysis of acetylcholine to acetate and choline.[16] One of the most important markers of AD disease is cholinergic loss.[17,18] AChE inhibitors strengthen central and peripheral cholinergic function by inhibiting the hydrolysis of ACh. Therefore, they are target molecules for treating AD disease.[13,19,20] Four clinically approved AChE inhibitors have been identified: tacrine, donepezil, rivastigmine, and galantamine.[10,21] However, the benefits of AChE inhibitor drugs available so far in clinical studies and practice are minimal, and due to their side effects, none of them have been fully successful.[13,22] Therefore, identifying new effective AChE inhibitors with less side effects has become a major requirement for treating AD. In previous studies, the AChE inhibition effect of many heterocyclic molecules, including quinazoline

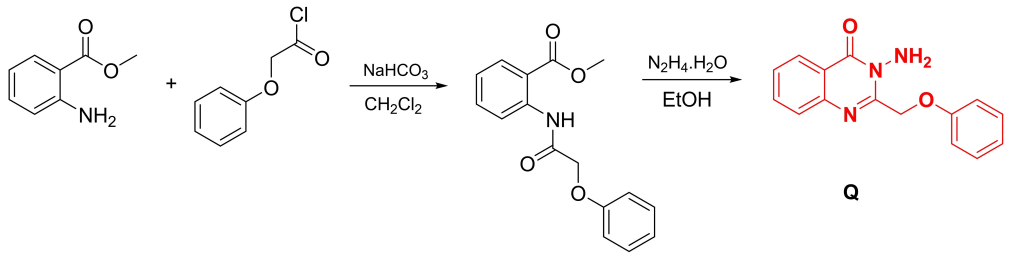

Scheme 1. Synthesis of compound **Q**.

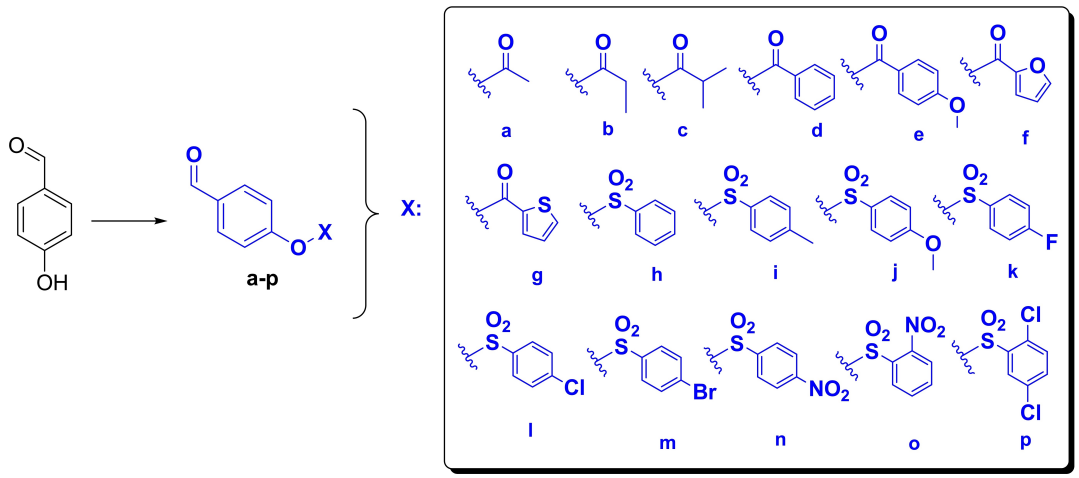

Scheme 2. Synthesis of compounds **a**–**p**.

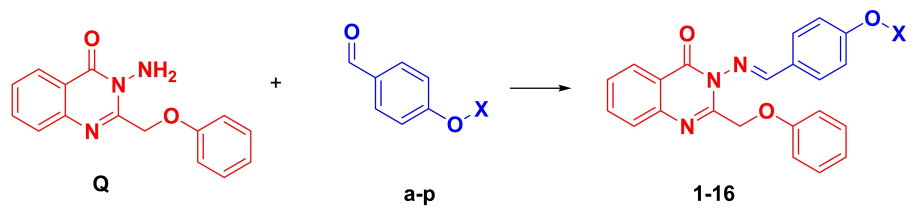

Scheme 3. Synthesis of compounds**1**–**16**.

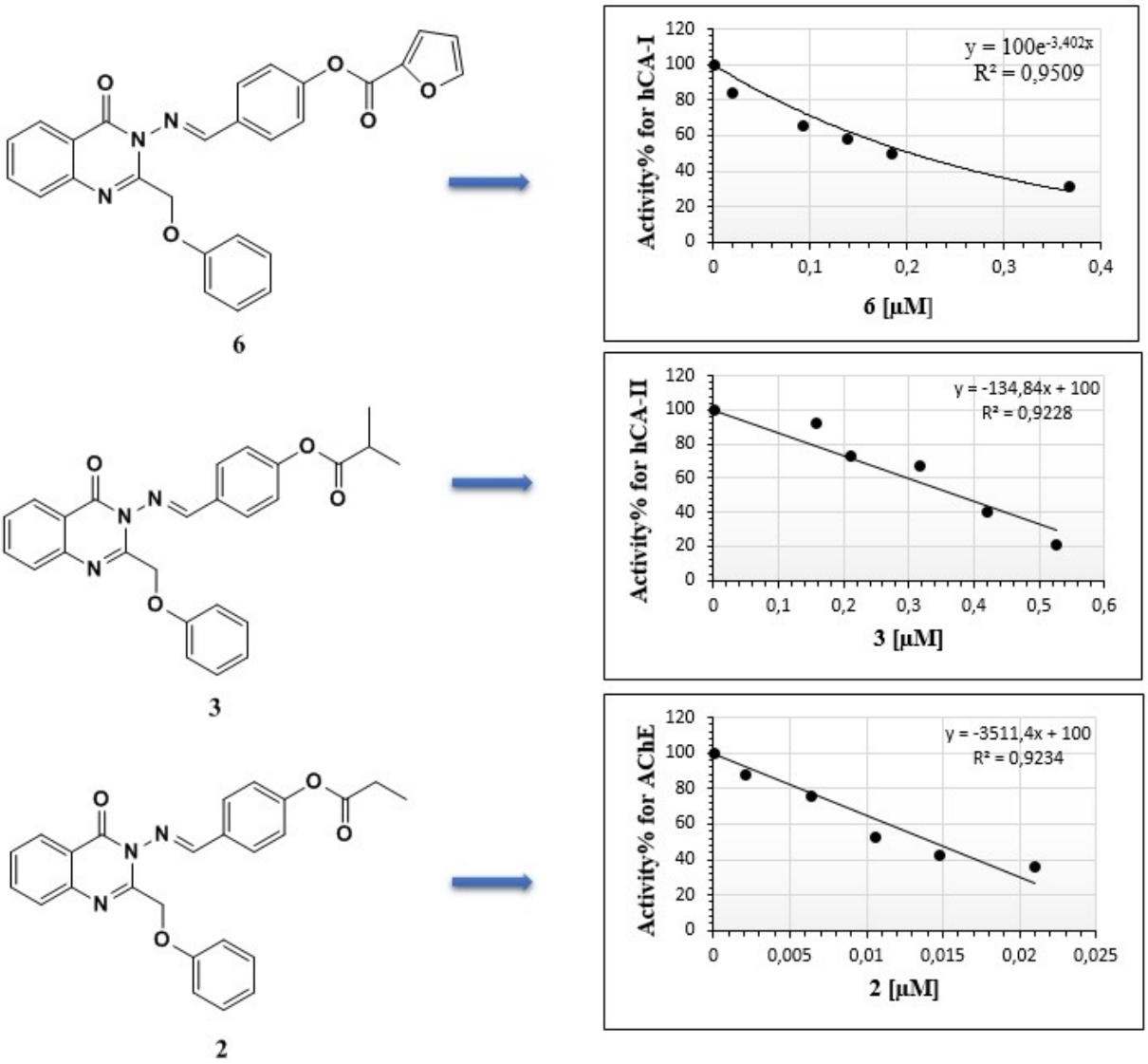

Figure 1. Molecules with the strongest inhibitory effect for hCA-I (**6**), hCA-II (**3**), and AChE (**2**) and their IC_{50} plots.

derivatives,[23] has been investigated and studies in this direction are continuing rapidly.

Quinazolines and quinazolinones are some of the common chemical building blocks belonging to the family of heterocyclic nitrogen compounds. Quinazoline is a heterocyclic compound formed from two fused six-membered simple aromatic rings, benzene and pyrimidine. Quinazolinones are the saturated form of the quinazolines and classified into three types according to the position and number of carbonyl group: 2(1*H*) quinazolinones, 4(3*H*) quinazolinones, and 2,4(1*H*,3*H*) quinazolindione. The accessibility of 4(3*H*) derivatives and the versatility of their biological activities attract attention to this class of compounds. There are many studies in the literature showing anticancer[24,25] antimicrobial,[26] anticonvulsant,[27]

Table 3. Important interactions and MolDock scores of **6**, **11**, and **12** derivatives in hCA-I active site.

Compounds	MolDock Score/ Ligand Efficiency	Category	Types	Interactions residues
6	−134.765/ −3.850	Hydrogen Bond	Carbon Hydrogen Bond	HIS200 GLN92
			Pi-Donor Hydrogen Bond	TRP5
		Electrostatic	Pi-Cation	ZN1
		Hydrophobic	Pi-Sigma	LEU198
			Pi–Pi Stacked	HIS200
			Pi–Pi T-shaped	TRP5
			Pi-Alkyl	PRO202 LEU131 ALA135 LEU198 VAL143
11	−127.722/ −3.361	Hydrogen Bond	Conventional Hydrogen Bond	GLN92 THR199
		Other	Metal-Acceptor	ZN
		Other	Pi-Sulfur	HIS94 TRP209
		Hydrophobic	Pi–Pi Stacked	PHE91 HIS200
			Pi-Sigma	LEU131 ALA135 VAL143
			Pi-Alkyl	LEU198 ALA121 LEU141 VAL207 LEU131
12	−128.122/ −3.133	Hydrogen Bond	Conventional Hydrogen Bond	GLN92 THR199
		Other	Metal-Acceptor	ZN
		Other	Pi-Sulfur	HIS94 HIS96 TRP209
		Hydrophobic	Pi-Sigma	LEU131
			Pi–Pi Stacked	HIS200
			Alkyl	ALA121 LEU141 VAL143
			Pi-Alkyl	LEU198 ALA121 LEU141 VAL143 LEU198 VAL207 LEU131

antihistaminic,[28] anti-inflammatory,[29] antileishmanial,[30] antioxidant and DNA protective,[31] antiviral,[32] anticholinergic[33] antidiabetic[34] and inhibitor of carbonic anhydrase[35,36] and acetylcholinesterase[23] properties of quinazolinone derivatives.

Due to the broad spectrum of biological activity of quinazolinones, chemists make various modifications to this compound class to obtain potent and highly selective agents. In this study, new quinazolin-4(3*H*)-one derivative was synthesized, and their reactions with acylated and sulfonylated phenolic aldehydes were investigated to determine new and potent inhibitors against hCA I–II and AChE.

Results and Discussion

Chemistry

In this study, thirty-three compounds were synthesized. Of these compounds, seventeen are intermediates (one novel and sixteen known) (Scheme 1 and 2), and sixteen are target novel molecules (Scheme 3). 3-amino-2-(phenoxymethyl) quinazolin-4(3*H*)-one (**Q**) was used as amine reactant. From the reactions of compounds **a**–**p** with **Q**, novel carboxylate and sulfonate derivatives containing quinazolin-3(4*H*)-one ring (**1**–**16**) were obtained with excellent yields (90-98%). The structures of the novel compounds were characterized with FTIR, ^{1}H NMR, ^{13}C NMR, and HRMS spectroscopic methods.

In the IR spectra of the compounds (**1**–**16**), the stretching bands of the aromatic and aliphatic C–H appeared at 3095–3034 cm^{-1} and 2979–2921 cm^{-1}, respectively. For compounds **1**–**7**, the stretching bands of C=O and the bending bands of C–O of carboxylate group were observed at 1757–1722 cm^{-1} and 1232–1205 cm^{-1}, respectively. For all compounds, C=O stretching bands of the quinazolinone ring were seen at 1682–1674 cm^{-1}. CH=N stretching bands of the benzylideneamino group appeared at 1598–1589 cm^{-1}. For compounds **8**–**16**, asymmetrical and symmetrical S=O stretching bands of SO_2 groups were seen at 1387–1366 and 1148–1143 cm^{-1}, respectively. For compounds **14** and **15**, bands of NO_2 groups appeared at 1548 and 1359, 1531 and 1346 cm^{-1}, respectively. These bands are the characteristic bands and the values are fully compatible with the structures and literature.[33,34]

In the ^{1}H NMR spectra of the compounds (**1**–**16**), peaks of N=CH protons appeared as a singlet at δ 9.25–9.18 ppm. Aromatic protons were observed at δ 8.38–6.61 ppm as a doublet, triplet, and multiplet relative to their chemical environment. Peaks of the phenoxymethyl ($PhOCH_2$-) protons at position 2 of the quinazolinone ring appeared as a singlet at δ 5.35–5.31 ppm. For compounds **5** and **10**, peaks of the

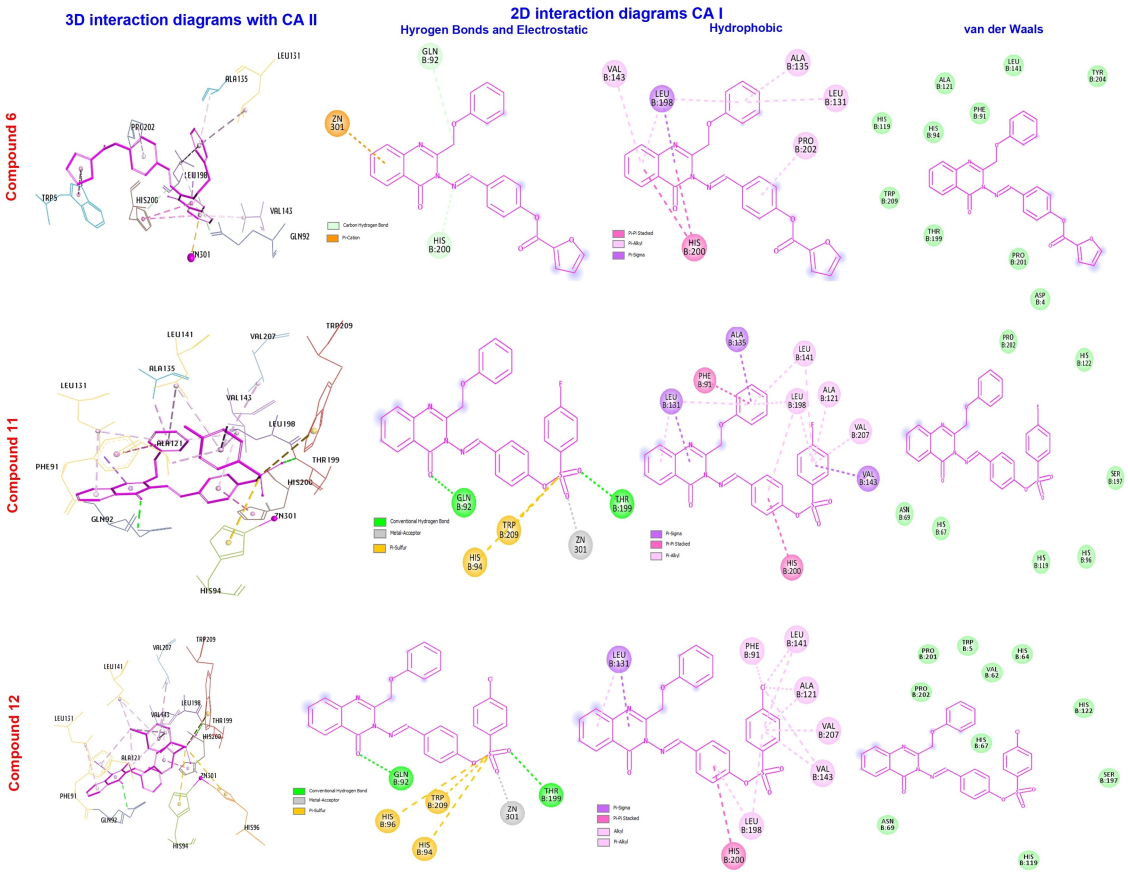

Figure 2. Representation of the interactions and positioning of compounds **6**, **11** and **12** in the binding site of hCA -I.

methoxy (OCH_3) protons resonated as a singlet at δ 3.89 and 3.88 ppm, respectively. For compound **1**, peak of the methyl protons of acetyl moiety was observed as a singlet at δ 2.32 ppm. For compound **2**, peaks of the ethyl protons of propionyl moiety were seen as a quartet at δ 2.61 ppm for -CH_2 and a triplet at δ1.27 ppm for -CH_3. Finally, for compound **3**, peaks of the isopropyl protons of isobutyl moiety appeared as a heptet at δ 2.82 ppm for -CH and a doublet at δ 1.33 ppm for two -CH_3. Chemical shifts, integrations, and splits are fully compatible with the structures and literature.[33,34]

In the ^{13}C NMR spectra of the new compounds (**1**–**16**), peaks of C=O carbons (ester and quinazolinone moiety) resonated at δ 175.0–164.8 ppm and δ 159.0–158.9 ppm, respectively. Peaks of C=N carbons of the quinazoline ring (C2) and CH=N carbons of benzylidenamino moieties were seen at δ 154.4–151.7 ppm and δ 165.0–163.5 ppm, respectively. Peaks of aromatic carbons resonated at δ 164.3–114.0 ppm. Peaks of the phenoxy methyl ($PhOCH_2$-) carbons at the position 2 of the quinazolinone ring were observed at δ 68.2–67.9 ppm. For compounds **5** and **10**, peaks of the methoxy carbons were seen at δ 55.8–55.6 ppm. For compounds **1**, peaks of the methyl carbons of acetyl moiety were observed at δ 21.2 ppm. For compound **2**, peaks of the ethyl carbons of propionyl moiety appeared at δ 27.8 ppm for -CH_2 and δ 9.0 ppm for -CH_3. Finally, for compound **3**, peaks of the isopropyl carbons of isobutyl moiety appeared at δ 34.2 ppm for -CH and δ 18.9 ppm for two -CH_3. Chemical shifts and the number of peaks are fully compatible with the structures and literature.[33,34]

Biological Activity Evaluation

The close association of CA isoenzymes with many physiological and pathological processes has made inhibitors of these isoenzymes the target molecules in drug design studies. Existing CA inhibitors have side effects and lack specificity, necessitating new CA inhibitors' discovery, and studies in this area are continuing rapidly.[11,22]

In present study the inhibition effects of new quinazoline-4(3*H*)-one derivatives (**1**–**16**) on hCA-I, hCA-II and AChE activities were investigated. Inhibitory effects of **1**–**16** compounds on hCA-I, hCA-II, and AChE activity were determined by IC_{50} (inhibitor concentration that halves the activity) values. IC_{50} values of **1**–**16** ranged from 205 nM to 3.32 μM for hCA-I. Molecule **6** (IC_{50}: 205 nM) showed the strongest inhibition effect on hCA-I (Figure 1), while molecule number **1** (IC_{50}: 3.32 μM) showed the lowest inhibition effect. **AZA** (IC_{50}: 476 nM) was used as the reference inhibitor for hCA-I. Molecules **6** (IC_{50}: 205 nM), **12** (IC_{50}: 282 nM), **11** (IC_{50}: 290 nM), **5** (IC_{50}: 342 nM), **13** (IC_{50}: 368 nM), **2** (IC_{50}: 371 nM) **9** (IC_{50}: 444 nM), **4** (IC_{50}: 453 nM),

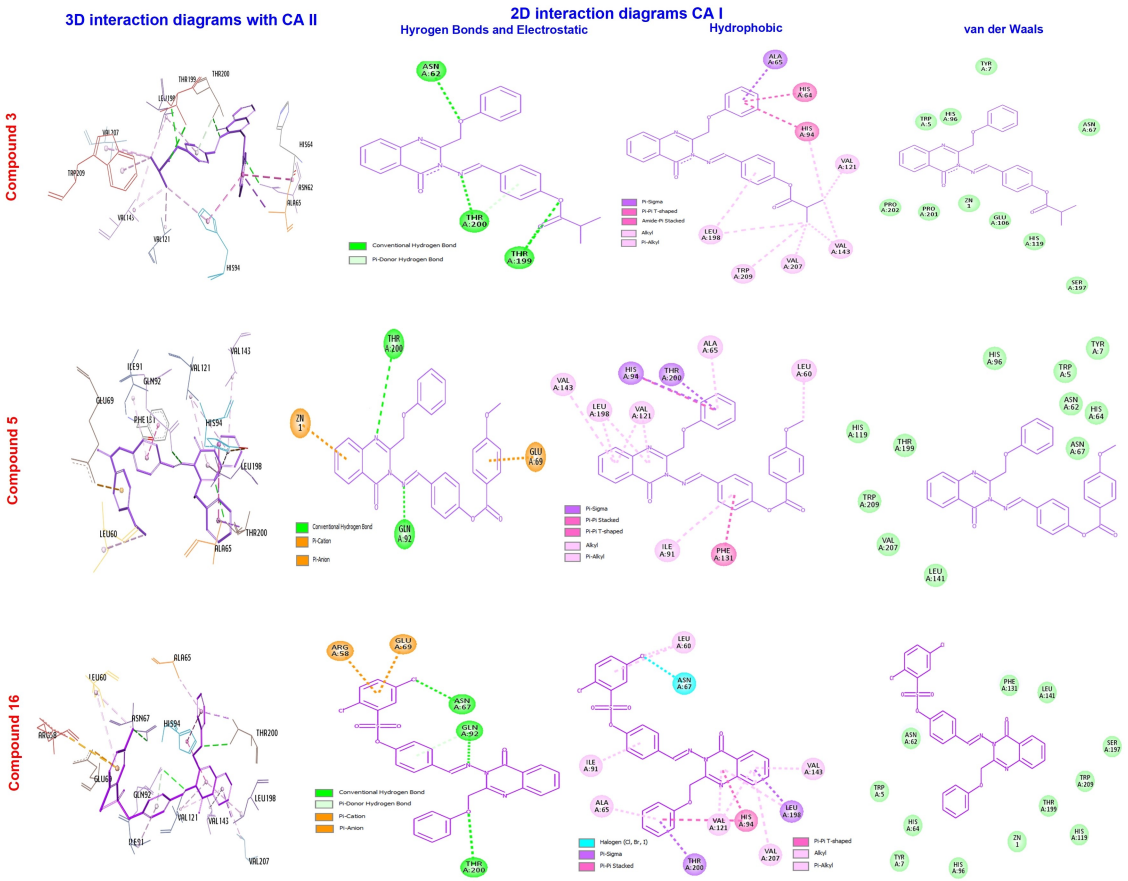

Figure 3. Representation of the interactions and positioning of compounds **3**, **5** and **16** in the binding site of hCA-II.

15 (IC_{50}: 453 nM) had more effective inhibition on hCA-I than **AZA**. The inhibition rate of molecule **14** (IC_{50}: 475 nM) was almost the same as **AZA**. Molecules **1** (IC_{50}: 3.32 μM), **3** (IC_{50}: 616 nM), **7** (IC_{50}: 592 nM), **16** (IC_{50}: 550 nM), **10** (IC_{50}: 518 nM), **8** (IC_{50}: 484 nM) had weaker inhibitory effect for hCA-I than AZA (Table 1). On the other hand, the IC_{50} values of molecules **1**–**16** were found in the 3.91 μM-209 nM range for hCA-II. While molecule **3** (IC_{50}: 209 nM) showed the strongest inhibition effect on hCA-II, molecule **1** (IC_{50}: 3.91 μM) showed the lowest inhibition effect. **AZA** (IC_{50}: 104 nM) was used as the reference inhibitor for hCA-II, and none of the molecules **1**–**16** had a stronger inhibitory effect for hCA-II than AZA. In the past, some studies showed that quinazoline-derived molecules had potent inhibitory effects on cytosolic isoenzymes hCA-I, hCA-II and tumor-associated trans-membrane enzymes hCA-IX, hCA-XII.[37] According to the results of this study, except for **1** of the **1**–**16**, which are the new quinazoline derivatives, other molecules exhibited strong inhibition effects on hCA-I and hCA-II at the nM level. Therefore, the results of this study will contribute to the literature on the determination of new quinazoline-derived CA inhibitors.

Most drug development studies for treating Alzheimer's disease have focused on AChE inhibition. On the other hand, quinazoline derivatives are important in the design and synthesis of drugs that act on the central nervous system.[23] For this reason, there are studies in the literature in which quinazoline derivatives are evaluated as AChE inhibitors.[13,23] The present study investigated the effects of new quinazoline derivatives (**1**–**16**) on AChE activity. All **1**–**16** molecules had an nM inhibition effect on AchE activity and were in the IC_{50} 14.2 nM–155 nM range. Tacrine (IC_{50}: 210 nM) was used as the reference inhibitor for AChE, and all molecules **1**–**16** had a much stronger inhibitory effect for AChE than Tacrine. For AChE, **2** (IC_{50}: 14.2 nM), (Figure 1) showed a strong inhibitory effect, and the inhibition effect of **2** was approximately 15 times greater than that of Tacrine. Although **13** (IC_{50}: 155 nM) had the weakest inhibitory effect on AChE compared to other molecules, its inhibition effect was stronger than Tacrine. The inhibition results of **1**–**16** for AChE are summarized in Table 2. In recent studies, the anti-AChE activities of a series of quinazoline-triazolehybrid compounds were evaluated.[13] It was determined that quinazoline derivative **1**–**16** molecules synthesized in this study had a powerful inhibition effect on AChE at the nM level and showed a better AChE inhibition effect than many quinazoline derivative molecules in the literature.[13]

Table 4. Important interactions and MolDock scores of **3**, **5**, and **16** derivatives in hCA-II active site.

Compounds	MolDock Score/ Ligand Efficiency	Category	Types	Interactions residues
3	−147.423/ −4.467	Hydrogen Bond	Conventional Hydrogen Bond	ASN62 THR199 THR200
			Pi-Donor Hydrogen Bond	THR200
		Hydrophobic	Alkyl	VAL207 LEU198 VAL143 VAL121
			Pi-Sigma	ALA65
			Pi–Pi T-shaped	HIS94
			Pi-Alkyl	HIS94 TRP209 LEU198
5	−143.142/ −3.766	Hydrogen Bond	Conventional Hydrogen Bond	GLN92 THR200
		Electrostatic	Pi-Cation	ZN1
			Pi-Anion	GLU69
		Hydrophobic	Pi–Pi T-shaped	HIS94
			Pi-Sigma	HIS94 THR200
			Alkyl	LEU60
			Pi-Alkyl	VAL121 LEU198 ILE91 ALA65 VAL143
16	−150.36/ −3.855	Hydrogen Bond;Halogen	Conventional Hydrogen Bond;Halogen	ASN67
		Hydrogen Bond	Conventional Hydrogen Bond	GLN92 THR200
			Pi-Donor Hydrogen Bond	GLN92
		Electrostatic	Pi-Cation	ARG58
		Electrostatic	Pi-Anion	GLU69
		Hydrophobic	Alkyl	LEU60
			Pi-Sigma	LEU198 THR200
			Pi–Pi Stacked	HIS94
			Pi–Pi T-shaped	HIS94
			Pi-Alkyl	VAL121 LEU198 ILE91 LEU60 ALA65 VAL121 VAL143 VAL207

Molecular Docking

Molecular docking study objects to understand the possible binding poses of the potential inhibitor compounds with the critical amino acids in the active site of the enzymes. The three most active compounds for each target were selected to predict their binding energies and the residues that interact with the enzymes.

The results obtained from the molecular modeling studies generally support the experimental results. However, sometimes there may be differences due to various reasons. Firstly, the percentages of docking programs to predict the correct docking positions are not one hundred percent. The program that gave the highest rate of correct attachment mode was used in this study.[38] Secondly, docking studies are done on frozen crystal structures of proteins. However, the behaviour of proteins and ligands in aqueous solutions is affected by different factors such as water molecules in the environment, buffer ions, lipophilicity and solubility of ligands. Third, the programs give the total interaction affinity values between protein and small molecules. Interaction with a vital amino acid in the catalytic region may contribute much more to the inhibition effect of the small molecule.[39] Therefore, ligand efficiency (LE) value, which expresses the ratio of affinity value to heavy molecules, was produced. Fourth, because larger molecules have much more functional groups, they can normally have a higher affinity value. However, this great structural feature can sometimes prevent it from settling in the active site, as well as preventing it from being sterically attached to the region in the appropriate conformation.[40]

The docking scores of **6**, **11**, and **12** with hCA-I were found to be −134.765, −127.722, and −128.122 MolDock Score, respectively, which agrees with *in vitro* inhibition results. The results and interaction detail are summarized in Table 3. Compound **6** formed carbon-hydrogen bonds with GLN92, HIS200 and a pi-donor hydrogen bond with TRP5. It indicated electrostatic (Pi-Cation: ZN1) and hydrophobic interactions (Pi-Sigma: LEU198; Pi–Pi Stacked: HIS200; Pi–Pi T-shaped: TRP5; Pi-Alkyl: PRO202, LEU131, ALA135, LEU198, VAL143). Compound **11** carved out hydrogen bonds with GLN92 and THR199, metal-acceptor interactions via ZN, and pi-sulfur bonds via HIS94 and TRP209. It demonstrated hydrophobic interactions (Pi–Pi

Table 5. Important interactions and MolDock scores of **1**, **2**, and **7** derivatives in AChE active site.

Compounds	MolDock Score/ Ligand Efficiency	Category	Types	Interactions residues
1	−175.344/ −5.656	Hydrogen Bond	Carbon Hydrogen Bond	GLY448 ASP74
			Pi-Donor Hydrogen Bond	TYR124
		Hydrophobic	Pi-Sigma	ASP74
			Pi–Pi Stacked	TRP286 TYR337 TYR341
			Pi–Pi T-shaped	TRP86 TYR124
2	−175.354/ −5.479	Hydrogen Bond	Conventional Hydrogen Bond	PHE295 ARG296
			Carbon Hydrogen Bond	HIS447 SER125
			Pi-Donor Hydrogen Bond	GLY121 SER125
		Hydrophobic	Pi–Pi Stacked	TRP86 TYR341
			Pi–Pi T-shaped	TYR124
			Pi-Alkyl	TRP286
7	−201.988/ −5.771	Hydrogen Bond	Conventional Hydrogen Bond	TYR124
			Pi-Donor Hydrogen Bond	SER125
		Electrostatic	Pi-Anion	ASP74
			Pi-Sigma	ASP74
		Hydrophobic	Pi–Pi Stacked	TRP86 TRP286 TYR337 TYR341
			Pi–Pi T-shaped	TRP86 TYR124

Stacked: PHE91, HIS200; Pi-Sigma: LEU131, ALA135, VAL143; Pi-Alkyl: LEU198, ALA121, LEU141, VAL207, LEU131). Compound **12** showed similar interactions as compound **11** (Figure 2).

The protein-ligand interaction profile and *in vitro* results spilled that compounds **3**, **5**, and **16** had the potential against the hCA-II. Figure 3 shows the binding mode of top poses at the hCA-II active site. Compound **3** effectuated four hydrogen bonds over residues ASN62, THR200, and THR199, besides hydrophobic interactions (Alkyl: VAL207, LEU198 VAL143, VAL121, VAL143, VAL121; Pi-Sigma: ALA65; Pi–Pi T-shaped: HIS94, Pi-Alkyl: HIS94, TRP209, LEU198). Compound **5** constructed hydrogen bonds with GLN92 and THR200. It conducted electrostatic (Pi-Cation: ZN1; Pi-Anion: GLU69) and hydrophobic (Pi–Pi T-shaped: HIS94; Pi-Sigma: HIS94, THR200; Alkyl: LEU60; Pi-Alkyl: VAL121, LEU198, ILE91, ALA65, VAL143) interactions. Compound **16** formed three types of hydrogen bonds (Conventional Hydrogen Bond, Halogen: ASN67; Conventional Hydrogen Bond: GLN92, THR200; Pi-Donor Hydrogen Bond: GLN92). Compound **16** showed the most hydrophobic interactions (Alkyl: LEU60; Pi-Sigma: LEU198, THR200; Pi–Pi Stacked: HIS94; Pi–Pi T-shaped: HIS94; Pi-Alkyl: VAL121, LEU198, ILE91, LEU60, ALA65, VAL121, VAL143, VAL207) compared to other compounds besides electrostatic interactions (Pi-Cation: ARG58; Pi-Anion: GLU69). Compounds for both enzymes formed numerous van der Waals interactions (Table 4).

Molecules interacted with crucial amino acids in the active sites of carbonic anhydrase enzymes, significantly contributing to the catalytic activity (Figures 2 and 3). The Zn(II) ion coordinated by three histidine residues (HIS 94, HIS 96, and HIS 119) was located in the center of the CAs active zone.[41] Compounds **6**, **11** and **12** interacted directly with the Zn(II) ion via Metal-Acceptor and electrostatic interactions to hCA-I while bound to histidine residues via hydrophobic interactions. It was reported that the GLN92 and THR199 amino residues of the carbonic anhydrase isoenzymes formed hydrogen bond interactions with potential sulfonamide inhibitors.[42] As seen in the tables and figures, similar to the reported study, hydrogen bonding appears to form between the sulfonyl group of compounds **11** and **12** and the residue of THR199, and the oxygen on the quinazolin-4-(3*H*)-one ring and GLN92 in interactions with hCA-I. *In vitro* and *in silico* results for CA I support each other. These results show that the estimated results of the Molegro Virtual Docker program may be close to reality.

Three compounds strongly interacting with hCA-II were also found in hydrogen bond interaction with Thr200 residue. In the interaction of hCA-II and molecules, it was seen that the active site makes hydrogen bond interactions with critical amino acids such as THR199 and THR200. Val 143 and Leu 198 are substrate-binding site amino acids at CAs.[43] It was

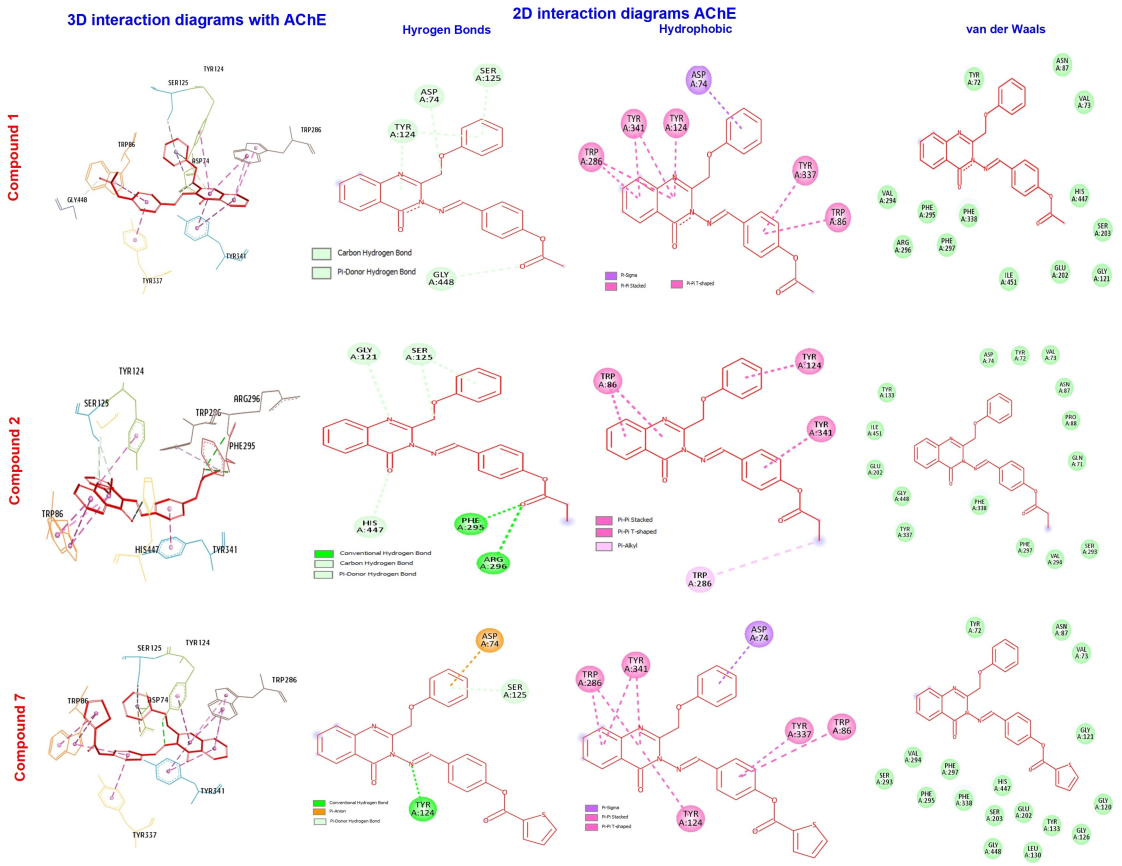

Figure 4. Representation of the interactions and positioning of compounds **1**, **2** and **7** in the binding site of AchE.

predicted that new molecules might bond via alkyl interactions with substrate-binding site amino acids such as VAL143 and LEU198 at hCA-I and hCA-II active regions. Although compound **3** has a lower MolDock score than compound **16**, it has both better LE value and the potential to interact with important acids such as ASN62, THR199, and THR200 in the active region with a very strong hydrogen bond. Therefore, it can have a better inhibition value. Compound **5** interacted directly with ZN, which is an important metal ion in enzyme activity. This may be the reason why it shows better activity than compound **16**.

The interactions of compounds **1**, **2**, and **7** and amino acids in the catalytic region of AChE are presented in Table 5. The view of protein-ligand interactions of the best poses is shown in Figure 4. As clearly depicted in Figure 4, with AChE; compound **1** formed hydrogen bonds (Carbon Hydrogen Bond: GLY448, ASP74; Pi-Donor Hydrogen Bond: TYR124) and showed hydrophobic interactions (Pi-Sigma: ASP74; Pi–Pi Stacked: TRP286, TYR337, TYR341; Pi–Pi T-shaped: TRP86, TYR124). Compound **2** constituted hydrogen bonds (Conventional Hydrogen Bond: PHE295, ARG296; Carbon Hydrogen Bond: HIS447, SER125, GLY121; Pi-Donor Hydrogen Bond: SER125); it made hydrophobic interactions (Pi–Pi Stacked: TRP86, TYR341; Pi–Pi T-shaped: TYR124; Pi-Alkyl: TRP286). Compound **7** effectuated hydrogen bonds bridge (Conventional Hydrogen Bond: TYR124; Pi-Donor Hydrogen Bond: SER125) established electrostatic (Pi-Anion: ASP74) and hydrophobic interactions (Pi-Sigma: ASP74; Pi–Pi Stacked: TRP86, TRP286, TYR337; Pi–Pi T-shaped: TRP86, TYR124). All three compounds showed multiple van der Waals interactions. The active site of acetylcholine esterase was well studied, and the amino acid residues to which the inhibitor and substrate bind were detailed.[44] Compound **2**, the best inhibition effect against this enzyme, made hydrogen bonds with HIS447 at the catalytic triad, PHE295 at the acyl pocket, and SER125 at the peripheral anionic site. It also performed Pi-Alkyl interaction with important amino acids from different regions, such as TYR124, TRP286, and PHE338, which were effective in inhibition. Therefore, its potent inhibition might also result from its perfect pairing with these amino acids. Compound **2** has a lower affinity score than compound **7**, but the strong inhibitory effect may be due to its more hydrogen bonding interactions with vital amino acids such as PHE295, HIS447, and SER125 in the catalytic site.

Conclusion

Considering the pharmacological importance of quinazolines due to their drug-like properties and the metabolic importance of CA and AChE inhibitors, the inhibition effects of the newly synthesized molecules on the hCA-I,II and AChE activities were

investigated. According to the results of this study, newly synthesized quinazolin-4(3*H*)-one (**1**–**16**) derivatives were evaluated as very potent inhibitors for AChE and hCAs. **6** and **3** were the molecules showing the most potent inhibitory effect for hCA-I and hCA-II, respectively, and even **6** had a nearly 2-fold more substantial inhibitory effect for hCA-I than AZA when looking at their IC_{50} values. On the other hand, molecules **1**–**16** all had a much stronger inhibitory effect for AChE than Tacrine, and **2** had an IC_{50} value about 15 times more effective than Tacrine with the strongest AChE inhibitor effect. Docking studies have shown that molecules have the potential to interact strongly with amino acids of catalytic importance in the active site of enzymes. In this context, it is thought that the results obtained in this study will contribute to studies on the design of new, effective CA and AChE inhibitors derived from quinazoline.

Experimental Section

Materials

The chemicals used in this study were supplied by Sigma Aldrich (Germany). Melting points were determined on WRS-2 A Microprocessor Melting-point Apparatus and are uncorrected. FTIR spectra of compounds were recorded using Alpha-P Bruker FT-IR Spectrophotometer. ^{1}H-NMR spectra were recorded on Bruker (400 MHz) spectrometer. ^{13}C-NMR spectra were recorded on Bruker (100 MHz) spectrometer. Chemical shifts were reported as δ in ppm relative to tetramethylsilane (TMS) (δ 0.00 singlet) in deuterated chloroform ($CDCl_3$). Healthy human erythrocytes used for the biological assays were received processed and anonymized from the University Blood Center, which follows the required ethical and consent guidelines in collecting samples.

Synthesis

Synthesis of 3-amino-2-(phenoxymethyl)quinazolin-4(3H)-one (Q)

The compound was synthesized using the method reported previously.[45] Sodium bicarbonate (20 mmol) was added to a solution of methyl anthranilate (10 mmol) in 20 mL dichloromethaneand the solution was stirred for 20 minutes at 0–5 °C. Phenoxyacetyl chloride (10 mmol) in 10 mL dichloromethane was added dropwise to this solution and stirred for an hour at room temperature. Reaction progress was monitored by TLC (Hex:EtOAc–9:1). The mixture was filtered off, and the solvent was removed under reduced pressure. The crude product (10 mmol) was dissolved in absolute ethanol (20 mL), and hydrazinium hydroxide (25 mmol, w/w: 80%) was added to this solution. The mixture was refluxed for 8 hours. Reaction progress was monitored by TLC (Hex:EtOAc–7:3). Half of the solvent was removed under reduced pressure, and diethylether (20 mL) was added. The mixture was left in the freezer overnight and formed white crystals were filtered off and washed with ice-cold ethanol (Scheme 1). ^{1}H NMR (400 MHz, $CDCl_3$) δ 8.26 (d, J = 8.0 Hz, 1H), 7.75 (d, J = 3.6 Hz, 2H), 7.50 (m, 1H), 7.31 (m,2H), 7.07 (d, J = 8.0 Hz, 2H), 7.02 (t, J = 7.3 Hz, 1H), 5.32 (s, 2H), 5.30 (s, 2H).

Synthesis of Compounds a–p

The compounds were synthesized using the method given by Tokalı *et al.*.[34] 4-hydroxybenzaldehyde (10 mmol) was dissolved in 20 ml THF, and the solution was put into an ice bath. Acyl chloride (for compounds **a**–**g**) or sulfonyl chloride (for compounds **h**–**p**) (10 mmol) was added to this solution in the cold. Triethylamine (11 mmol) in 10 mL THF was added to the solution dropwise and stirred for 30 minutes at room temperature. After refluxing for three hours, the solvent was removed under reduced pressure. The formed residue was washed with cold water and recrystallized from ethanol (Scheme 2).

Synthesis of Target Compounds (1–16)

To a solution of compound **Q** (10 mmol) in glacial aceticacid (6 mL), compounds **a**–**p** (10 mmol) were added and refluxed for an hour. The solvent was evaporated, and crude products were recrystallized from ethanol (Scheme 3). The physical properties, the FTIR, NMR, and HRMS spectra of the compounds **1**–**16** and the data obtained from these spectra were provided in the Supporting Information section.

Biological Activity StudiesInhibition Studies on hCA-I and hCA-II

Healthy human erythrocytes used for the biological assays were received processed and anonymized from the Atatürk University Blood Center, which follows the required ethical and consent guidelines in collecting samples. hCA-I and hCA-II were isolated from human erythrocytes using the CNBr-activated Sepharose-4B-L-tyrosine sulfanilamide affinity chromatography method.[2,46] During the isolation of isoenzymes, quantitative protein determination was made by the Bradford method,[47] and the purity of isoenzymes was checked by the SDS-PAGE method.[48] hCA-I and hCA-II isoenzymes were purified by affinity chromatography dialyzed against 50 mM Tris-SO4 (pH 7.4) buffer overnight. After dialysis, isoenzymes were stored in small fractions of one milliliter at −80 °C for use in inhibition studies. In inhibition studies, the activities of hCA-I and hCA-II isoenzymes were performed according to the esterase activity measurement method.[49] In this method, CA hydrolyzes the p-nitrophenolacetate used as a substrate to p-nitrophenol and acetic acid, and the resulting p-nitrophenol absorbs at 348 nm. Accordingly, p-nitrophenyl acetate was used as the substrate in the inhibition studies. The formation of p-nitrophenol from p-nitrophenyl acetate was monitored by measuring the absorbance at 348 nm, 25 °C using a spectrophotometer. The enzyme unit was calculated using the absorption coefficient ($\varepsilon = 5.4 \times 10^3\ M^{-1} cm^{-1}$) of p-nitrophenyl acetate at 348 nm.[22] Inhibition effects of 1–16 molecules were determined on the esterase activity of hCA-I and II isoenzymes. For this, hCA-I and hCA-II activities were measured at least five concentrations of each molecule. Percent activity values of both isoenzymes at five different inhibitor concentrations were calculated. The control activity of the enzyme was accepted as 100%, and inhibitor concentrations were graphed versus the percent activity of both isoenzymes. IC_{50} values were determined from the equations of these graphs. Acetazolamide (AZA) was the reference inhibitor for hCA-I and hCA-II isoenzymes.

Inhibiton Studies on AChE

In the present work, AChE from the electrical eel (Electrophorus electricus) (CAS no. 9000–81-1) enzyme was commercially available from Sigma-Aldrich. AChE activity in inhibition studies was

performed according to the spectrophotometric method of Ellman *et al.*.[50] The basis of this method is as follows: Acetylthiocholine iodide is used as substrate. AChEcatalyzes the conversion of acetylthiocholine to thiocholine and acetic acid. The thiocholine formed due to the reaction with the DTNB (Ellman's reagent, 5.5-dithio-bis-(2-nitrobenzoic acid) added to the reaction medium during the activity measurement. As a result of this reaction, a yellow-colored 5-thio-2-nitrobenzoic acid complex is formed. The color intensity of the resulting colored compound is measured spectrophotometrically.[46,21] Accordingly, acetylthiocholine iodide was used as a substrate in inhibition studies. The color intensity of the resulting colored compound was measured at 412 nm. AChE activity was measured at least five concentrations for **1–16** compounds to determine the inhibition effects of **1–16** on AChE activity. The control activity of the enzyme was accepted as 100%, and inhibitor concentrations were graphed against Activity%. IC_{50} values were determined from the equations of these graphs. Tacrine (TAC) was used as the reference inhibitor for AChE.

Molecular Docking

In this study, molecular modeling study was performed for the three molecules that showed the strongest inhibitory effect on hCA-I, hCA-II and AChE activity.In order to predict the docking of molecules in the active sites of enzymes, docking studies were performed using the Molegro Virtual Docker software.[51] The Experimentally-determined X-ray crystal structures of CA-I, CA-II, and AChE were retrieved from the RCSB Protein Data Bank (RCSB PDB) website with 6G3 V, 3PO6, and 4EY7 PDB IDs, respectively.[52,53,54] The 2D structures of the synthesized molecules were drawn in Chemdraw and transferred to the MarvinSketch program for checking as structure and obtaining the 3D SDF structures. Molegro Virtual Docker performed regularization and optimization for enzymes and new molecules in docking studies. A grid box with the coordinates of the crystal ligands in the center was created at the active site of the enzymes. Ten trials were performed at the active sites of the targets for each molecule. The high-scoring poses were selected and were visualized and analyzed using Discovery Studio Visualizer.

Supporting Information Summary

The yields, physical and spectral data and the spectra (FTIR, NMR, and HRMS) of the synthesized new compounds were given in the supporting information file.

Author Contribution Statement

Synthesis studies were carried out by F.S. Tokalı, Z. Alım carried out biological activity studies and molecular docking studies were carried out by Ü. Yırtıcı. Analysis of the results was done by F.S. Tokalı, Z. Alım and Ü. Yırtıcı. The writing and language correction of the article were done by F.S. Tokalı, Z. Alım and Ü. Yırtıcı.

Conflict of Interest

The authors declare no conflict of interest.

Data Availability Statement

The data that support the findings of this study are available in the supplementary material of this article.

Keywords: Acetylcholinesterase · carbonic anhydrase · docking · inhibition · Schiff base · quinazolin-4(3*H*)-one

[1] S. Kumar, S. Rulhania, S. Jaswal, V. Monga, *Eur. J. Med. Chem.* **2021**, *209*, 112923.
[2] D. Ekinci, S. Beydemir, Z. Alım, *Pharmacol. Rep.* **2007**, *59*, 580–587.
[3] C. T. Supuran, *J. Enzyme Inhib. Med. Chem.* **2016**, *31*, 345–360.
[4] E. R. Buabeng, M. Henary, *Bioorg. Med. Chem.* **2021**, *39*, 116140.
[5] M. Hamide, Y. Gök, Y. Demir, G. Yamalı, T. K. Tok, A. Aktaş, R. Sevincek, B. Güzel, İ, Gülçin, *J. Mol. Struct.* **2022**, *1265*, 133266.
[6] E. Karakılıç, Z. Alım, M. Emirik, A. Baran, *Appl. Organomet. Chem.* **2022**, *36*, e6537.
[7] S. Çol, M. Emirik, Z. Alım, A. Baran, *Appl. Organomet. Chem.* **2022**, *36*, e6799.
[8] C. T. Supuran, A. Scozzafava, *Expert Opin. Ther. Pat.* **2000**, *10*, 575–600.
[9] C. T. Supuran, A. Scozzafava, *Bioorg. Med. Chem.* **2007**, *15*, 4336–4350.
[10] Z. Köksal, Z. Alım, S. Bayrak, İ. Gülçin, H. Özdemir, *J. Biochem. Mol. Toxicol.* **2019**, *33*, e22300.
[11] Z. Alım, Z. Köksal, M. Karaman, *Pharmacol. Rep.* **2020**, *72*, 1738–1748.
[12] Z. Najafi, M. Mahdavi, M. Saeedi, E. Karimpour-Razkenari, R. Asatouri, F. Vafadarnejad, F. H. Moghadam, M. Khanavi, M. Sharifzadeh, T. Akbarzadeh, *Eur. J. Med. Chem.* **2017**, *125*, 1200–1212.
[13] G. Le-Nhat-Thuy, N. N. Thi, H. Pham-The, T. A. D. Thi, H. N. Thi, T. H. N. Thi, S. N. Hoang, T. V. Nguyen, *Bioorg. Med. Chem. Lett.* **2020**, *30*, 127404.
[14] R. Dai, Y. Sun, R. Su, H. Gao, *Biomed. Pharmacother.* **2022**, *154*, 113576.
[15] M. Gümüş, Ş. N. Babacan, Y. Demir, Y. Sert, İ. Koca, İ. Gülçin, *Arch. Pharm.* **2022**, *355*, 2100242.
[16] M. Schumacher, S. Camp, Y. Maulet, M. Newton, K. MacPhee-Quigley, S. S. Taylor, T. Friedmann, P. Taylor, *Comp. Stud.* **1986**, *319*, 407–409.
[17] S. Manzoor, M. T. Gabr, B. Rasool, K. Pal, N. Hoda, *Biochem.* **2021**, *116*, 105354.
[18] M. Son, C. Park, S. Rampogu, A. Zeb, K. Woo Lee, *Int. J. Mol. Sci.* **2019**, *20*, 1000.
[19] V. Pejchal, S. Stepankova, M. Pejchalova, K. Kralovec, M. Lepsik, *Bioorg. Med. Chem.* **2016**, *24*, 1560–1572.
[20] A. Asghar, M. Yousuf, G. Fareed, R. Nazir, A. Hassan, A. Maalik, T. Noor, N. Iqbal, L. Rasheed, *RSC Adv.* **2020**, *10*, 19346–19352.
[21] H. Shirinzadeh, E. Dilek, Z. Alım, *ChemistrySelect* **2022**, *7*, e202104489.
[22] Z. Alım, T. Tunç, N. Demirel, A. Günel, N. Karacan, *J. Mol. Struct.* **2022**, *1268*, 133647.
[23] Z. Haghighijoo, L. Zamani, F. Moosavi, S. Emami, *Eur. J. Med. Chem.* **2022**, *227*, 113949.
[24] H. A. Mahdy, M. K. Ibrahim, A. M. Metwaly, A. Belal, A. B. M. Mehany, K. M. A. El-Gamal, A. El-Sharkawy, M. A. Elhendawy, M. M. Radwan, M. A. Elsohly, I. H. Eissa, *Bioorg. Chem.* **2020**, *94*,103422.
[25] M. N. Noolvi, H. M. Patel, V. Bhardwaj, A. Chauhan, *Eur. J. Med. Chem.* **2011**, *46*, 2327–2346.
[26] G. Naganagowda, A. Petsom, *J. Sulfur Chem.* **2011**, *32*, 223–233.
[27] H. M. Patel, M. N. Noolvi, A. A. Shirkhedkar, A. D. Kulkarni, C. V. Pardeshi, S. J. Surana, *RSC Adv.* **2016**, *6*, 44435–44455.
[28] V. Alagarsamy, P. S. Sundar, M. Gobinath, S. Nivedhitha, P. Parthiban, D. Shankar, M. T. Sulthana, V. R. Solomon, *Med. Chem. Res.* **2013**, *22*, 2486–2492.
[29] D. B. Farag, N. A. Farag, A. Esmat, S. A. Abuelezz, E. A. Ibrahim, D. A. El-Ella, *MedChemComm* **2015**, *6*, 283–299.
[30] M. Arfan, R. Khan, M. A. Khan, S. Anjum, M. I. Choudhary, M. Ahmad, *J. Enzyme Inhib. Med. Chem.* **2010**, *25*, 451–558.
[31] S. Kuntikana, C. Bhat, M. Kongot, S. I. Bhat, A. Kumar, *ChemistrySelect* **2016**, *1*, 1723–1728.
[32] X. Gao, X. Cai, K. Yan, B. Song, L. Gao, Z. Chen, *Molecules* **2007**, *12*, 2621–2642.
[33] F. S. Tokalı, P. Taslimi, I. H. Demircioğlu, M. Karaman, M. S. Gültekin, K. Şendil, I. Gülçin, *Arch. Pharm.* **2021**, *354*, e2000455.

[34] F. S. Tokalı, Y. Demir, I. H. Demircioğlu, C. Türkeş, E. Kalay, K. Şendil, Ş. Beydemir, *Drug Dev. Res.* **2022**, *83*, 586–604.
[35] A. S. El-Azab, A. M. Alaa, S. Bua, A. Nocentini, M. A. El-Gendy, M. A. Mohamed, T. Z. Shawer, N. A. AlSaif, C. T. Supuran, *Bioorg. Chem.* **2019**, *87*, 78–90.
[36] A. S. El-Azab, A. A. M. Abdel-Aziz, H. E. A. Ahmed, S. Bua, A. Nocentini, N. A. AlSaif, A. J. Obaidullah, M. M. Hefnawy, C. T. Supuran, *J. Enzyme Inhib. Med. Chem.* **2020**, *35*, 598–609.
[37] A. M. Alafeefy, R. Ahmad, M. Abdulla, W. M. Eldehna, A. M. Al-Tamimi, H. A. Abdel-Aziz, O. Al-Obaid, F. Carta, A. A. Al-Kahtani, C. T. Supuran, *Eur. J. Med. Chem.* **2016**, *109*, 247–253.
[38] J. De Azevedo, F. Walter, *Curr. Drug Targets* **2010**, *11*, 327–334.
[39] C. H. Reynolds, B. A. Tounge, S. D. Bembenek, *J. Med. Chem.* **2008**, *51*, 2432–2438.
[40] P. W. Kenny, *J. Cheminformatics* **2019**, *11*, 8.
[41] C. T. Supuran, *Nat. Rev. Drug Discovery* **2008**, *7*, 168–181.
[42] F. Abbate, A. Casini, A. Scozzafava, C. T. Supuran, *J. Enzyme Inhib. Med. Chem.* **2003**, *18*, 303–308.
[43] F. Briganti, S. Mangani, P. Orioli, A. Scozzafava, G. Vernaglione, C. T. Supuran, *Biochemistry* **1997**, *36*, 10384–10392.
[44] T. Furqan, S. Batool, R. Habib, M. Shah, H. Kalasz, F. Darvas, K. Kuca, E. Nepovimova, S. Batool, S. M. Nurulain, *Biomol. Eng.* **2020**, *10*, 758.
[45] F. S. Tokalı, *ChemistrySelect* **2022**, *7(48)*, e202204019.
[46] Z. Alım, N. Kilinç, M. M. Işgör, B. Şengül, Ş. Beydemir, *Chem. Biol. Drug Des.* **2015**, *86*, 857–863.
[47] M. M. Bradford, *Anal. Biochem.* **1976**, *72*, 248–254.
[48] U. K. Laemmli, *Nature* **1970**, *227*, 680–685.
[49] J. A. Verpoorte, S. Mehta, J. T. Edsall, *J. Biol. Chem.* **1967**, *242*, 4221–4229.
[50] G. L. Ellman, K. D. Courtney, V. Andres Jr, R. M. Featherstone, *Biochem. Pharmacol.* **1961**, *7*, 88–95.
[51] R. Thomsen, M. H. Christensen, *J. Med. Chem.* **2006**, *49*, 3315–3321.
[52] P. Mader, J. Brynda, R. Gitto, S. Agnello, P. Pachl, C. T. Supuran, A. Chimirri, P. Rezacova, *J. Med. Chem.* **2011**, *54*, 2522–2526.
[53] J. Cheung, M. J. Rudolph, F. Burshteyn, M. S. Cassidy, E. N. Gary, J. Love, M. C. Franklin, J. J. Height, *J. Med. Chem.* **2012**, *55*, 10282–10286.
[54] A. Angeli, M. Ferraroni, C. T. Supuran, *ACS Med. Chem. Lett.* **2018**, *9*, 1035–1038.

Submitted: October 29, 2022
Accepted: February 8, 2023